Letter

Circularly Polarized Plasmons in Chiral Gold Nanowires via Quantum-Mechanical Design

Daniele Toffoli, Andrea Russi, Giovanna Fronzoni, Emanuele Coccia, Mauro Stener,* Luca Sementa, and Alessandro Fortunelli*

Cite This: https://doi.org/10.1021/acs.jpclett.1c01364

Read Online

ACCESS | 📊 Metrics & More | 📖 Article Recommendations | 🔵 Supporting Information

ABSTRACT: Time-dependent density functional theory (TDDFT) simulations are conducted on a series of chiral gold nanowires to explore whether an enhancement of circular dichroism at the plasmon resonance is possible and identify its quantum-mechanical origin. We find that in linear two-dimensional chiral nanowires the dichroic response is suppressed by destructive interference of nearly degenerate components with opposite signs, pointing to this phenomenon as a common and likely origin of the difficulty encountered so far in achieving a plasmonic CD response in experiment and suggesting nevertheless that these opposite components could be "decoupled" by using multiwall arrangements. In contrast, we predict a giant dichroic response for nanowires with three-dimensional helical coiling. We rationalize this finding via an electronic structure analysis of longitudinal and transversal plasmonic excitations and their coupling into chiral components, and we propose a simple formula for the chiral response as a function of structural parameters (nanowire length and coiling number).
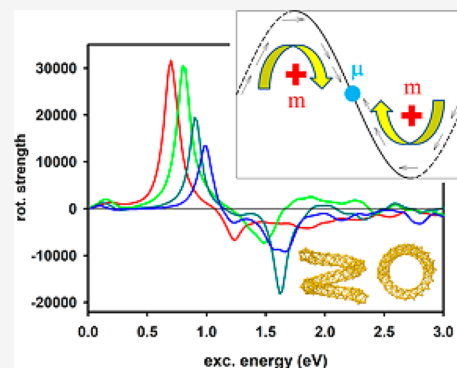
Plasmons are of paramount importance in nanotechnology due to their ability of focusing the electromagnetic field with a high energy density in a small region of space[1−3] and are nowadays routinely employed in enhanced spectroscopic techniques such as surface-enhanced Raman spectroscopy,[4] allowing detection down to single-molecule spectroscopic signals.[5,6] Although the nature of these excitations is well understood for extended systems as a collective motions of conduction band electrons, for finite nanostructured systems such as nanoclusters and nanowires their physics is still debated.[7−11]

When the system is chiral, a nonzero a circular dichroism (CD) signal is expected. The CD response can be exploited to achieve extremely selective chiral sensing.[12] However, the CD signal, being governed by an electric-dipole/magnetic-dipole scalar product (the Rosenfeld equation),[13] is much weaker than absorption, typically by a factor of $\approx 10^{-5}$. Enhancing CD via plasmonic effects is therefore a very appealing possibility and has been the subject of many studies in the past decade.[14−17] Plasmonic CD can be classified into structural and induced CD,[17] according to its being based either on systems that are inherently chiral (structural CD)[18] or on the chiral arrangement of nonchiral systems (induced CD). Induced plasmonic CD seems more accessible at the experimental level,[19] but interest for structural chiral plasmonics is exponentially growing due to the widened synthetic possibilities achieved via new bottom-up advanced techniques. In particular, hot electrons can promote chiral growth mechanisms in nanocrystals, as also supported by

theoretical modeling.[20] Moreover, the interaction of circularly polarized light with plasmonic gold nanoresonators can allow one to discriminate hot-electron transfer.[21] Despite the interest arisen by these new developments, the experimentally observed plasmonic CD enhancements are so far not striking. We believe that this is due to the fact that the principles of both structural and induced plasmonic CD, which could guide the design of optimal nanostructures, are still scarcely known.

The goal of this work is to derive building principles of structural plasmonic CD in chiral Au gold nanowires from quantum-mechanical (QM) modeling so as to arrive at a rational design of and full exploitation of the possibilities provided by this class of systems. Via predictive time-dependent density-functional theory (TDDFT) simulations,[22−24] we show that a huge chiral plasmonic enhancement can be achieved in nanowires coiled in 3D arrangements, at the same time interpreting it in terms of an electronic structure analysis of longitudinal and transversal plasmonic excitations and their coupling into chiral components and providing simple working estimates. In contrast, we find that an analogous potential enhancement in linear systems is likely

69 to be suppressed by destructive interference among excitations
70 from the different regions of the system, and we suggest that
71 this phenomenon is a probable origin of the difficulty
72 experienced so far in achieving an intense plasmonic CD
73 response. However, we suggest that it is possible to overcome
74 the latter issues and retrieve a strong plasmonic CD response
75 also in linear arrangements by properly tuning the system
76 morphological features so as to avoid destructive interference
77 phenomena.

78   To predict chiro-optical spectra of nanowires, we employ the
79 polTDDFT[22−24] approach and analyze its results via individual
80 component map—oscillator strength plots (ICM-OS),[25] ICM−
81 rotator strength plots (ICM-RS),[26] and a geometrical model to
82 assess plasmonic behavior (computational details can be found
83 in the Supporting Information). The polTDDFT method has
84 proven very efficient for applications on large systems, with
85 deviations of the peak positions within at most 0.2 eV with
86 respect to reference Casida calculations.[22]

87   Figure 1 illustrates schematic atomistic depictions of the
88 gold nanowires considered in this work; more details about
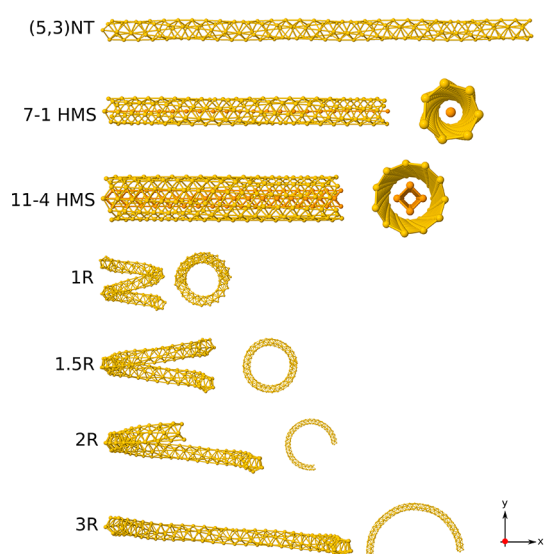

Figure 1. Structures of the Au clusters considered in the present work.

89 their structures can be found in the Supporting Information.
90 We start our analysis from the linear chiral nanowires in the
91 upper panel, such systems are the most similar to the ones
92 produced experimentally.[27] Although these systems are linear,
93 they are still chiral as a result of the arrangement of the external
94 atoms along their longitudinal axis (z direction in Figure 1).
95 The photoabsorption of the three chiral nanotubes is reported
96 in panel a of Figure 2: the profiles display a single sharp
97 plasmon which is blue-shifted as the length of the nanowires
98 decreases. However, in the rotatory strength plots reported in
99 panel b of Figure 2, we do not observe any dichroic peak in
100 correspondence of the plasmons for the Au(5,3) SWNT and
101 for the 7-1 HMS. For the 11-4 HMS a double peak at around
102 1.9−2.0 eV with opposite polarity does appear, although with a
103 maximum rotator strength much weaker than those we could
104 expect and will find below in the helical systems. The ICM-RS
105 plots for the three structures calculated in correspondence of
106 the plasmon peak and reported in panels c−f of Figure 2 allow
107 us to rationalize immediately this behavior. The plots are
108 typically plasmonic, with major off-diagonal contributions.

109 Strikingly, however, two spots very close to each other (nearly
110 degenerate) with opposite sign and a very high absolute value
111 are apparent: for more clarity, in panel f of Figure 2 we
112 reproduce as a 3D plot the ICM-RS 2D plot of panel e
113 highlighting opposite contributions canceling each other. This
114 means that the CD response in these systems is nearly totally
115 suppressed as a result of a destructive interference of the
116 magnetic dipole moment contributions of the excited
117 configurations, mixed as a consequence of the collective
118 nature of the plasmon.

119   The presence of two opposite peaks suggests the possibility
120 of "decoupling" them via an external perturbation and thus
121 enhance the resulting CD signal. This possibility is supported
122 by the plots reported in Figure S5 where the 11-4 HMS
123 photoabsorption and CD spectra are compared with those
124 calculated separately for its constituent walls: the inner
125 nonchiral (4,2) nanotube (NT) and the outer chiral (11,6)
126 NT. Both the single-wall and the multishell NTs display strong
127 plasmons, increasing in energy in going from inner to outer
128 (empty) and the multishell NTs. The plasmon dichroism is
129 naturally absent for the (4,2) NT but is present in both (11,6)
130 NT and the 11-4 HMS. What is noteworthy is that the
131 plasmon dichroism is increased by a factor of 3 in going from
132 the single-wall (11,6) NT to the multishell structure, which is
133 surprising since the inner system is not chiral at all. This
134 demonstrates that the presence of the inner NT, although
135 achiral, plays the role of a "perturbation" able to amplify the
136 dichroic signal of a chiral structure and suggests the possibility
137 of further enhancing this amplification, for example, going to
138 multiwall nanotubes with increasing number of walls. Another
139 possibility in this respect could be to use ligands able to
140 electronically interact with the plasmonic system. The
141 conclusion of this investigation is anyway that the CD signal
142 of linear systems is non-negligible only when a perturbing
143 effect decoupling the two peaks with opposite sign in the ICM-
144 RS plots producing destructive interference in the chiro-optical
145 plasmonic response is present in the structure. Could this be
146 achieved and the CD signal be plasmonic-enhanced in
147 intrinsically chiral single-component Au nanostructures? To
148 answer the question, we now turn to the photoabsorption and
149 CD spectra of the four helical structures: 1R, 1.5R, 2R, and 3R
150 of Figure 1.

151   Figure 3 reports the photoabsorption spectra (upper panel)
152 of the four helical structures here investigated, all with a length
153 of 82 Å. In the helix with the smallest radius (1R) we find two
154 weak plasmonic peaks at 0.70 and at 1.24 eV followed by two
155 other maxima at 1.92 and 2.60 eV. As the helix/nanowire is
156 coiled with increasing radius, the spectral features evolve in
157 two ways. (i) The first peak grows exponentially in intensity
158 and is blue-shifted, where the progression in energy is 0.70,
159 0.82, 0.94, and 1.00 eV, and the oscillator strengths change as f
160 = 0.85, 2.8, 9.3, and 23.6. (ii) The second peak displays a
161 similar blue-shift behavior, but the trend in intensity is not
162 monotonic and a maximum in intensity is reached for the 2R
163 system, where the progression in energy is 1.24, 1.60, 1.62, and
164 1.70 eV and in the oscillator strength is f = 0.73, 9.7, 15.7, and
165 8.4. The plasmonic nature of the peaks is confirmed by ICM-
166 OS plots reported in the Supporting Information. The rapidly
167 growing intensity with increasing size of the system is indeed
168 typical of plasmonic behavior.

169   In the lower panel of Figure 3 the CD spectra of the four
170 helical structures are reported, expressed as rotation strength
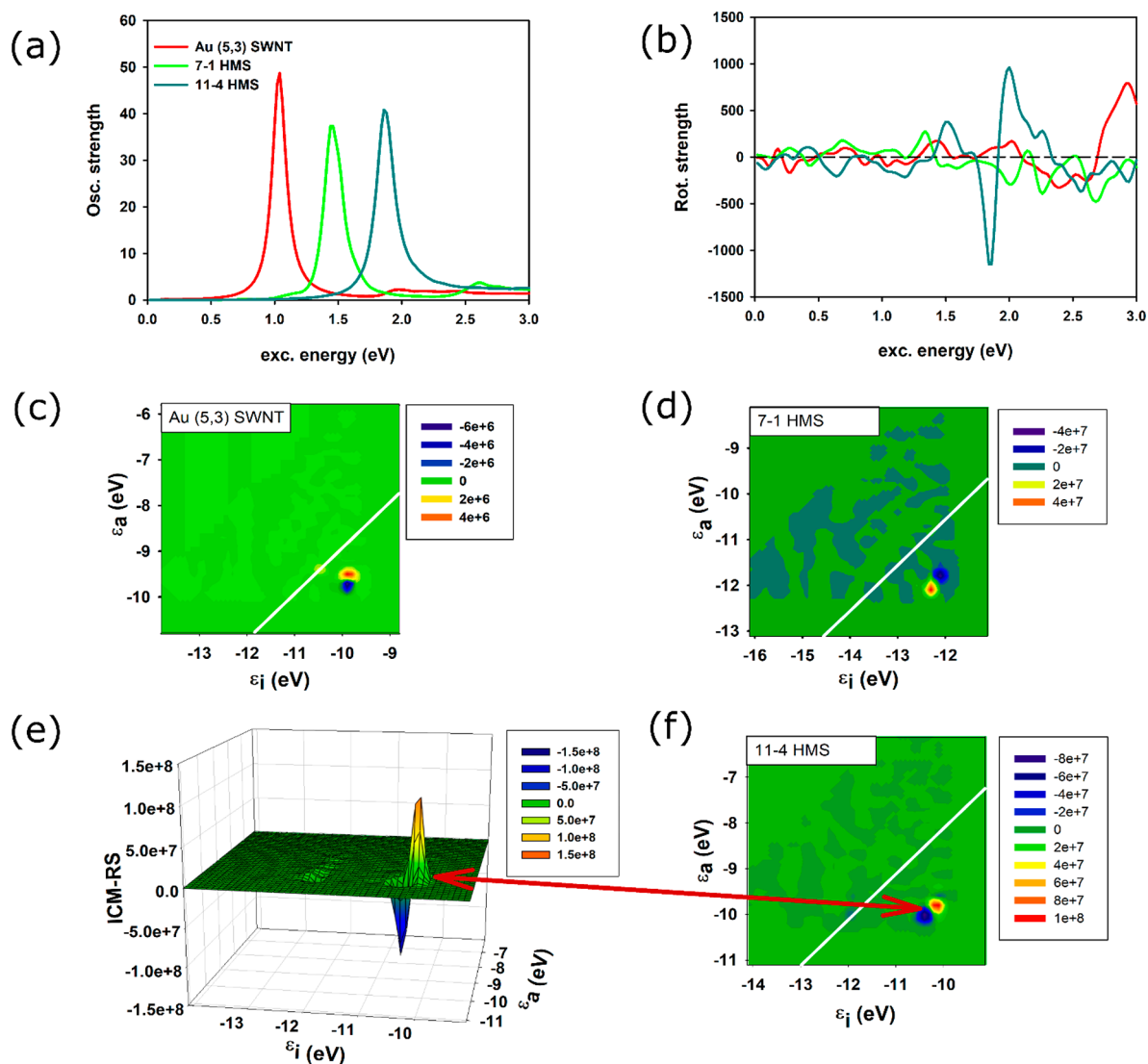171 (R), given by the Rosenfeld equation as the imaginary scalar

Figure 2. Photoabsorption (a) and CD (b) for the series of linear chiral nanotubes. ICM-RS analysis for the series of linear chiral nanotubes: (c) at 1.04 eV, (d) at 1.44 eV, and (e, f) at 1.86 eV. Oscillator strengths are given in atomic units, while R is given in 10^{-40} esu^2 cm^2. In the ICM-RS plots, ε_i and ε_a are the energies of the occupied and virtual molecular orbitals, respectively, in eV. Note that the ICM-RS scale is different in the various panels.

product between the electric ($\boldsymbol{\mu}$) and magnetic ($\mathbf{m}$) dipole transition moments:

$$R = \mathrm{Im}\ \boldsymbol{\mu} \cdot \mathbf{m} \qquad (1)$$

Two spectral features are apparent in Figure 3, counterparts of the photoabsorption peaks at approximately the same excitation energies. Interestingly, for all clusters the dichroism is positive for the lower energy feature whereas the higher energy peak has negative polarity. For the lower energy peak, the trend observed in the CD is different from that observed in absorption, with a similar intensity for 1R and 1.5R nanowires and a decrease for the larger radii. In contrast, the band of negative polarity at higher energy follows approximately behavior of photoabsorption, growing in intensity with increasing radius up to the 2R helix and then weakening to lower intensity in the 3R structure. It is worth noting that a similar behavior has been predicted by classical electrodynamics for much larger helices (with pitch up to 70 nm and radius of 20 nm) where two plasmons of opposite sign were found.[20] Because the present systems are much smaller,

the importance of quantum size effects prevents the use of classical approaches in favor of TDDFT. Note that the CD signal of our coiled nanowires is much stronger than that of our linear nanowires, at least by a factor of 30: a giant CD is thus found in intrinsically chiral single-component Au nanowires.

Analysis of the physical origin of the CD behavior of the helical systems can be achieved via geometrical considerations (here we use arguments from the analysis of helicenes[28]). We can imagine that electrons flow following the electromagnetic field in plasmon resonances. When a right-handed helix with longitudinal plasmon field is considered (upper panel of Figure 4), the current goes from left to right, producing an accumulation of charge that generates an electric-dipole transition moment from left to right. The current also promotes a magnetic dipole transition moment, and since the current flows along a right-handed helix, the magnetic-dipole transition moment vector also points from left to right, thus being parallel to the electric-dipole moment. Because the Rosenfeld equation (eq 1) contains a scalar product between
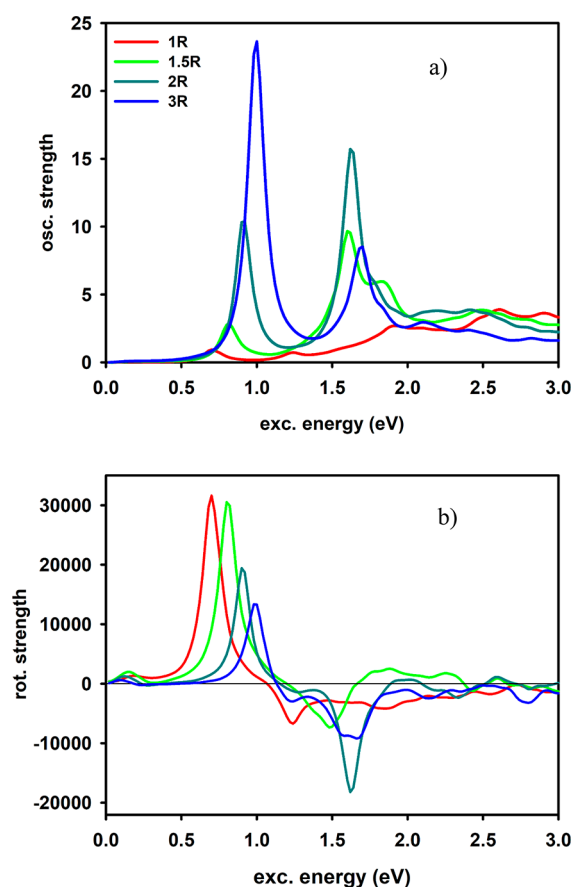
C

Figure 3. Photoabsorption (upper panel) and CD (lower panel) for the series of the four helices with increasing radius considered in this work. Oscillator strengths are given in atomic units, while R is given in 10^{-40} esu^2 cm^2.
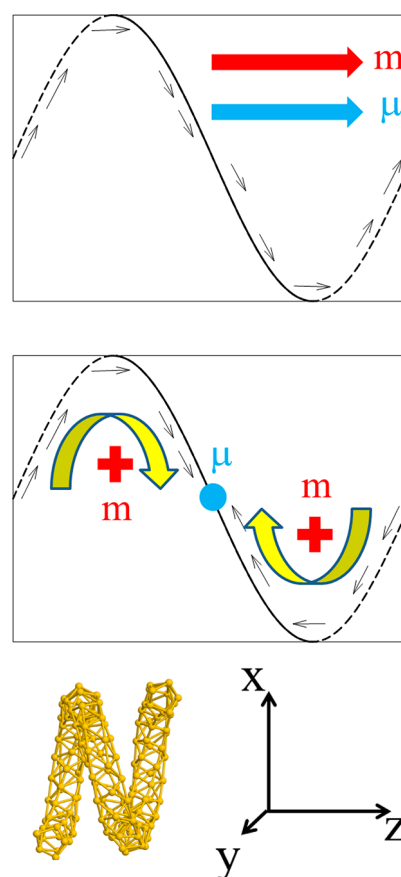

Figure 4. Scheme of induced current as well as electric and magnetic dipole for longitudinal (upper panel) and transversal (lower panel) plasmons. See the text for details.

the electric and magnetic dipole transition moments, the contribution to the dichroism is positive in this case. When a transversal plasmon field (lower panel of Figure 4) perpendicular to the figure emerging form the plane (as the y axis in the figure) is considered, the charge flows following the field and accumulates in the center of the helix creating an electric dipole transition moment along the y direction. Now let us consider the contribution of the two branches of current: if they are observed with respect to the y direction, they appear as two left-handed helices, so the magnetic dipole transition moment will have opposite sign with respect to the electric dipole, giving a negative contribution to the dichroism. In summary, from simple geometric considerations and by viewing a plasmon as a current oscillation along the helix, we expect a positive contribution from longitudinal and a negative one from transversal plasmons.

This conclusion is corroborated by looking at the Cartesian components to the CD spectra. We obtain longitudinal and transversal contributions by splitting oscillator and rotator strength spectra according to their Cartesian dipole component (x, y, and z). Having in mind the orientation of the helices (Figure 1), x and y are the transversal components and z is the longitudinal one. The decomposition of photoabsorption and CD spectra for the four helices is presented in Figure 5. Starting with the dichroism of the 1R helix (upper right panel), the positive plasmonic dichroic signal at 0.7 eV is contributed only by the z-component, while a weaker negative signal at 1.24 eV is found to be associated with the y-

component, and the x-component gives rise to a broad structure around 2 eV. The evolution of the dichroism along the series (panels on the right side of Figure 5) allows us to provide guiding principles. For the lower-energy band the strong contribution of the z-component hardly changes intensity along the series. On the contrary, the contribution of the transversal components, that is negative, rapidly gains strength and gives rise to an increasing cancellation with the strong positive z-contribution. The apparent decrease in *average* rotatory strength from 1R to 3R in Figure 3b (where we report the isotropic average of Cartesian components) is therefore understood simply as the consequence of a cancellation between a large, positive, and constant longitudinal z-component and a progressively increasing negative transversal y- or x-component that can be rationalized, as we will see in the next paragraph, in terms of the coiling number of the nanowire. We conclude that a giant dichroic response can be obtained in helical nanowires at low energies, whose rotatory strength intensity is approximately proportional to the length of the nanowire minus cancellation effects in the *average* response due to limited coiling that can increase the transversal components opposing the longitudinal one. Note that the physical origin of these cancellation effects is different from electronic interference discussed for the linear systems and in particular that they *disappear when spatial symmetry is broken* in anisotropic systems.

We observe in passing that for the 3R helix the observed behavior can be rationalized by simple geometric arguments. From Figure 1 it is apparent that the size of the system along x
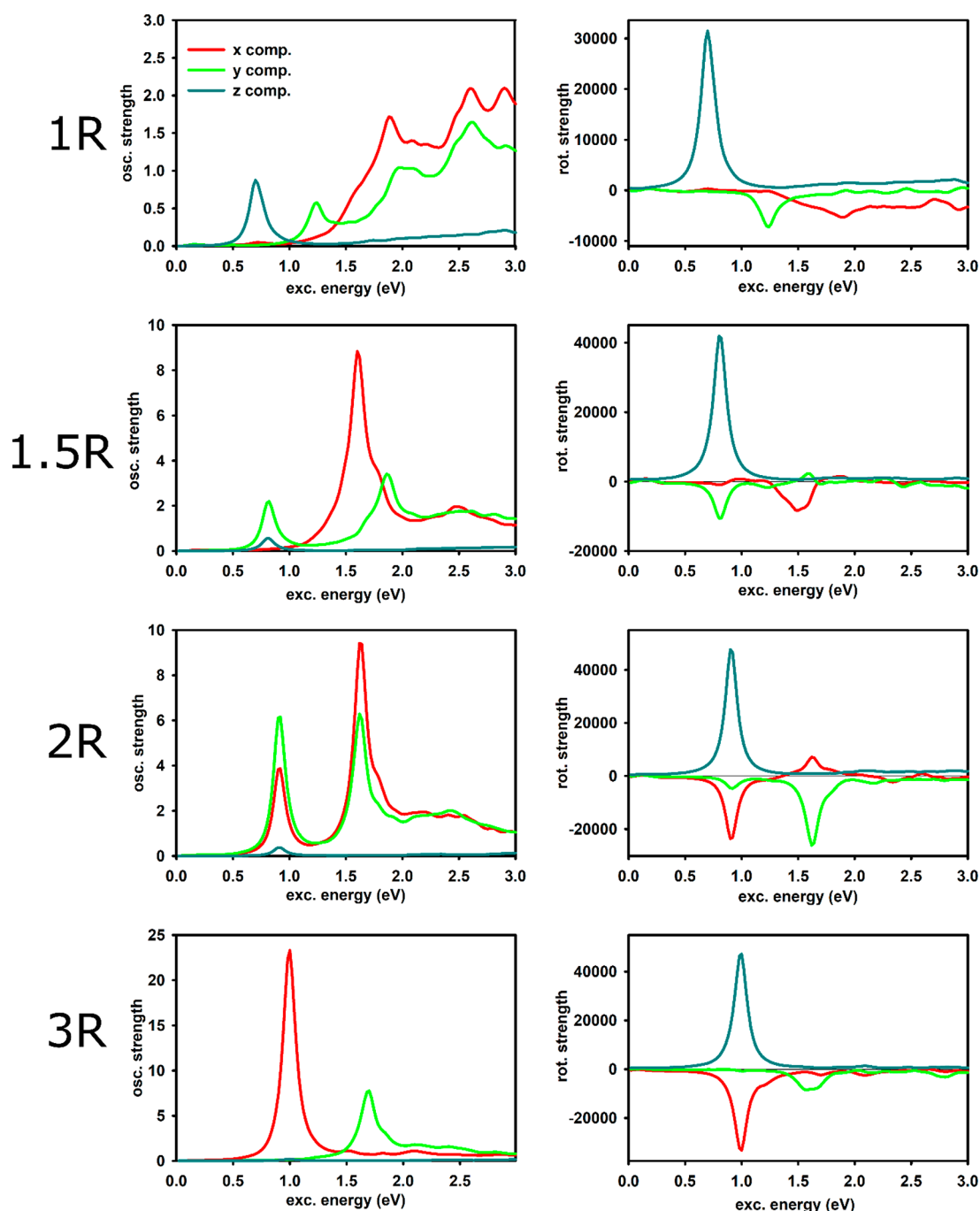
Figure 5. Partial contribution according to dipole components of photoabsorption (left panels) and circular dichroism (right panels) for the series of the four helices with increasing radius. f is given in atomic units and R in 10^{-40} esu^2 cm^2.

is roughly twice that along the y direction, and accordingly the plasmon along x is red-shifted and more intense with respect to that found along y, in agreement with calculated profiles of both oscillator f and rotatory R strength (see lower panels of Figure 5). For the other clusters the rationalization is less straightforward and is discussed in section 3 of the Supporting Information.

To summarize, in this work we employ accurate TDDFT simulations to predict the chiro-optical spectra of a series of gold chiral nanowires with helical or linear structure. We can answer the question of whether it is possible to achieve an enhanced dichroic response in correspondence with the plasmon resonance. We find that linear chiral nanotubes do

not exhibit a strong dichroic response. We trace back the suppression of chirality in the linear case to a destructive interference phenomenon and suggest "decoupling" the opposite components, for example, by increasing the thickness of multiwall structures or by employing ligands interacting with the plasmon as a way to recover a plasmonic CD. In contrast, a giant dichroic response is found for nanowires with helical structure. Via an analysis of the plasmonic resonance and of the origin of dichroism in both linear and helical systems, we provide an *ab initio* theoretical understanding and guiding principles of chiral plasmonics in metal nanowires. In particular, in helical nanowires we rationalize dichroic response as the sum of positive longitudinal and negative transversal

components, with the former proportional to the length and the latter function of the winding number of the wires. Such principles represent an operative tool to guide rational design of this class of systems and its applications, for example, in photocatalysis[29] for asymmetric synthesis or for sensors targeting a specific enantiomer.

■ ASSOCIATED CONTENT

Ⓢ Supporting Information

The Supporting Information is available free of charge at https://pubs.acs.org/doi/10.1021/acs.jpclett.1c01364.

> PolTDDFT theoretical method, computational details, definitions of ICM-OS and ICM-RS analysis, cluster structures, induced densities, ICM-OS plots, ICM-RS plots, and linear chiral nanotubes spectra (PDF)

■ AUTHOR INFORMATION

Corresponding Authors

Mauro Stener − *Dipartimento di Scienze Chimiche e Farmaceutiche, Università di Trieste, 34127 Trieste, Italy;* ⓞ orcid.org/0000-0003-3700-7903; Email: stener@units.it

Alessandro Fortunelli − *CNR-ICCOM & IPCF, Consiglio Nazionale delle Ricerche, 56124 Pisa, Italy;* ⓞ orcid.org/0000-0001-5337-4450; Email: alessandro.fortunelli@cnr.it

Authors

Daniele Toffoli − *Dipartimento di Scienze Chimiche e Farmaceutiche, Università di Trieste, 34127 Trieste, Italy;* ⓞ orcid.org/0000-0002-8225-6119

Andrea Russi − *Dipartimento di Scienze Chimiche e Farmaceutiche, Università di Trieste, 34127 Trieste, Italy*

Giovanna Fronzoni − *Dipartimento di Scienze Chimiche e Farmaceutiche, Università di Trieste, 34127 Trieste, Italy;* ⓞ orcid.org/0000-0002-5722-2355

Emanuele Coccia − *Dipartimento di Scienze Chimiche e Farmaceutiche, Università di Trieste, 34127 Trieste, Italy;* ⓞ orcid.org/0000-0003-3389-0989

Luca Sementa − *CNR-ICCOM & IPCF, Consiglio Nazionale delle Ricerche, 56124 Pisa, Italy*

Complete contact information is available at:
https://pubs.acs.org/10.1021/acs.jpclett.1c01364

Notes

The authors declare no competing financial interest.

■ ACKNOWLEDGMENTS

■ REFERENCES

(1) Zhang, C.; Noguez, J. Z. Plasmonic Optical Properties and Applications of Metal Nanostructures. *Plasmonics* **2008**, *3*, 127−150.

(2) Rycenga, M.; Cobley, C. M.; Zeng, J.; Li, W.; Moran, C. H.; Zhang, Q.; Qin, D.; Xia, Y. Controlling the Synthesis and Assembly of Silver Nanostructuresfor Plasmonic Applications. *Chem. Rev.* **2011**, *111*, 3669−3712.

(3) Durante, N.; Fortunelli, A.; Broyer, M.; Stener, M. Optical properties of Au nanoclusters from TD-DFT calculations. *J. Phys. Chem. C* **2011**, *115*, 6277−6282.

(4) Langer, J.; Jimenez de Aberasturi, D.; Aizpurua, J.; Alvarez-Puebla, R. A.; Auguié, B.; Baumberg, J. J.; Bazan, G. C.; Bell, S. E. J.; Boisen, A.; Brolo, A. G.; et al. Present and Future of Surface-Enhanced Raman Sattering. *ACS Nano* **2020**, *14*, 28−117.

(5) Barbry, M.; Koval, P.; Marchesin, F.; Esteban, R.; Borisov, A. G.; Aizpurua, J.; Sánchez-Portal, D. Atomistic Near-Field Nanoplasmonics: Reaching Atomic-Scale Resolution in Nanooptics. *Nano Lett.* **2015**, *15*, 3410−3419.

(6) Sementa, L.; Marini, A.; Barcaro, G.; Negreiros, F. R.; Fortunelli, A. Atomistic Quantum Plasmonics of Gold Nanowire Arrays. *ACS Photonics* **2014**, *1*, 315−322.

(7) Bernadotte, S.; Evers, F.; Jacob, C. R. Plasmons in molecules. *J. Phys. Chem. C* **2013**, *117*, 1863−1878.

(8) Zhang, R.; Bursi, L.; Cox, J. D.; Cui, Y.; Krauter, C. M.; Alabastri, A.; Manjavacas, A.; Calzolari, A.; Corni, S.; Molinari, E.; et al. How To Identify Plasmons from the Optical Response of Nanostructures. *ACS Nano* **2017**, *11*, 7321−7335.

(9) Sinha-Roy, R.; García-González, P.; Weissker, H.-C.; Rabilloud, F.; Fernández-Domínguez, A. I. Classical and ab Initio Plasmonics Meet at Sub-nanometric Noble Metal Rods. *ACS Photonics* **2017**, *4*, 1484−1493.

(10) Mokkath, J. H.; Schwingenschlögl, U. Optical properties of Al nanostructures from time dependent density functional theory. *J. Chem. Phys.* **2016**, *144*, 134305.

(11) Halas, N. J.; Lal, S.; Chang, W.-S.; Link, S.; Nordlander, P. Plasmons in Strongly Coupled Metallic Nanostructures. *Chem. Rev.* **2011**, *111*, 3913−3961.

(12) Kameta, N.; Masuda, M.; Shimizu, T. Qualitative/chiral sensing of amino acids by naked-eye fluorescence change based on morphological transformation and hierarchizing in supramolecular assemblies of pyrene-conjugated glycolipids. *Chem. Commun.* **2015**, *51*, 11104−11107.

(13) Pelayo, J. J.; Valencia, I.; García, A. P.; Chang, L.; López, M.; Toffoli, D.; Stener, M.; Fortunelli, A.; Garzón, I. L. Chirality in bare and ligand-protected metal nanoclusters. *Adv. Phys.: X* **2018**, *3*, 1509727.

(14) Karimova, N.; Aikens, C. M. Time-Dependent Density Functional Theory Investigation of the Electronic Structure and Chiroptical Properties of Curved and Helical Silver Nanowires. *J. Phys. Chem. A* **2015**, *119*, 8163−8173.

(15) Nguyen, L.; Dass, M.; Ober, M. F.; Besteiro, L. V.; Wang, Z. M.; Nickel, B.; Govorov, A. O.; Liedl, T.; Heuer-Jungemann, A. Chiral Assembly of Gold-Silver Core-Shell Plasmonic Nanorods on DNA Origami with Strong Optical. *ACS Nano* **2020**, *14*, 7454−7461.

(16) Slocik, J. M.; Dennis, P. B.; Govorov, A. O.; Bedford, N. M.; Ren, Y.; Naik, R. R. Chiral Restructuring of Peptide Enantiomers on Gold Nanomaterials. *ACS Biomater. Sci. Eng.* **2020**, *6*, 2612−2620.

(17) Hu, Z.; Meng, D.; Lin, F.; Zhu, X.; Fang, Z.; Wu, X. Plasmonic Circular Dichroism of Gold Nanoparticle Based Nanostructures. *Adv. Opt. Mater.* **2019**, *7*, 1801590.

(18) Fan, Z.; Govorov, A. O. Chiral Nanocrystals: Plasmonic Spectra and Circular Dichroism. *Nano Lett.* **2012**, *12*, 3283−3289.

(19) Zeng, C.; Chen, Y.; Liu, C.; Nobusada, K.; Rosi, N. L.; Jin, R. Gold tetrahedra coil up: Kekulé-like and double helical superstructures. *Sci. Adv.* **2015**, *1* (9), No. e1500425.

(20) Khorashad, L. K.; Besteiro, L. V.; Correa-Duarte, M. A.; Burger, S.; Wang, Z. M.; Govorov, A. O. Hot Electrons Generated in Chiral Plasmonic Nanocrystals as a Mechanism for Surface Photochemistry and Chiral Growth. *J. Am. Chem. Soc.* **2020**, *142*, 4193−4205.

(21) Fang, Y.; Verre, R.; Shao, L.; Nordlander, P.; Käll, M. Hot Electron Generation and Cathodoluminescence Nanoscopy of Chiral Split Ring Resonators. *Nano Lett.* **2016**, *16*, 5183−90.

(22) Baseggio, O.; Fronzoni, G.; Stener, M. A new time dependent density functional algorithm for large systems and plasmons in metal clusters. *J. Chem. Phys.* **2015**, *143*, 024106.

(23) Baseggio, O.; De Vetta, M.; Fronzoni, G.; Toffoli, D.; Stener, M.; Sementa, L.; Fortunelli, A. Time-Dependent Density-Functional Study of the Photoabsorption Spectrum of [Au25(SC2H4C6H5)18]

anion: validation of the computational protocol. *Int. J. Quantum Chem.* **2018**, *118*, No. e25769.

(24) Baseggio, O.; Toffoli, D.; Fronzoni, G.; Stener, M.; Sementa, L.; Fortunelli, A. Extension of the Time-Dependent Density Functional Complex Polarizability Algorithm to Circular Dichroism: Implementation and Applications to Ag8 and Au38(SC2H4C$_6$H$_5$)24. *J. Phys. Chem. C* **2016**, *120*, 24335−24345.

(25) Theivendran, S.; Chang, L.; Mukherjee, A.; Sementa, L.; Stener, M.; Fortunelli, A.; Dass, A. Principles of Optical Spectroscopy of Aromatic Alloy Nanomolecules: Au36-xAgx(SPh-tBu)24. *J. Phys. Chem. C* **2018**, *122*, 4524−4531.

(26) Chang, L.; Baseggio, O.; Sementa, L.; Cheng, D.; Fronzoni, G.; Toffoli, D.; Aprà, E.; Stener, M.; Fortunelli, A. Individual Component Map of Rotatory Strength and Rotatory Strength Density plots as analysis tools of circular dicroism spectra of complex systems. *J. Chem. Theory Comput.* **2018**, *14*, 3703−3714.

(27) Oshima, Y.; Onga, A.; Takayanagi, K. Helical Gold Nanotube Synthesized at 150 K *Phys. Rev. Lett.* **2003**, *91*, 205503.

(28) Furche, F.; Ahlrichs, R.; Wachsmann, C.; Weber, E.; Sobanski, A.; Vogtle, F.; Grimme, S. Circular Dichroism of Helicenes Investigated by Time-Dependent Density Functional Theory. *J. Am. Chem. Soc.* **2000**, *122*, 1717−1724.

(29) Zhou, L.; Martirez, J. M. P.; Finzel, J.; Zhang, C.; Swearer, D. F.; Tian, S.; Robatjazi, H.; Lou, M.; Dong, L.; Henderson, L.; et al. Light-driven methane dry reforming with single atomic site antenna-reactor plasmonic photocatalysts. *Nature Energy* **2020**, *5*, 61−70.